Ubiquity of Optical Activity in Planar Metamaterial Scatterers

Ivana Sersic,* Marie Anne van de Haar, Felipe Bernal Arango, and A. Femius Koenderink
Center for Nanophotonics, FOM Institute for Atomic and Molecular Physics (AMOLF), Science Park 104, 1098 XG Amsterdam, The Netherlands
(Received 13 January 2012; published 30 May 2012)

Recently it was discovered that periodic lattices of metamaterial scatterers show optical activity, even if the scatterers or lattice show no 2D or 3D chirality, if the illumination breaks symmetry. We demonstrate that such ''pseudochirality'' is intrinsic to any single planar metamaterial scatterer and in fact has a well-defined value at a universal bound. We argue that in any circuit model, a nonzero electric and magnetic polarizability derived from a single resonance automatically imply strong bi-anisotropy, i.e., magnetoelectric cross polarizability at the universal bound set by energy conservation. We confirm our claim by extracting polarizability tensors and cross sections for handed excitation from transmission measurements on near-infrared split ring arrays, and electrodynamic simulations for diverse metamaterial scatterers.

DOI: 10.1103/PhysRevLett.108.223903 PACS numbers: 42.70.−a, 42.25.−p, 78.20.Ci

Unresolved questions on how to rigorously describe the effective electrodynamic response of media composed of subwavelength building blocks currently acquire new relevance in nano-optics. Initiated by the works of Veselago and Pendry [1], efforts are focused on manipulating effective medium parameters in nanostructured metamaterials. On the one hand, the drive for arbitrary ϵ and μ is generated by the idea that light fields can be arbitrarily reshaped by conformal transformations, provided we can create arbitrary constitutive tensors [2]. On the other hand, a convergence with plasmonics has led to the realization that subwavelength scatterers greatly enhance rich scattering phenomena known from molecular matter [3,4]. For example, resonantly induced optical magnetism in 2D and 3D chiral metal nano-objects results in giant circular birefringence, optical rotatory power, broadband optical activity, and circular dichroism in frequency ranges from microwave, mid-IR, to even visible frequencies [5]. The fact that strong optical activity is easily attained using chiral or even achiral [6] subwavelength scatterers is promising for many applications such as broadband optical components, as well as for achieving negative refraction [7], or repulsive Casimir forces [8]. Moreover, the promise of enhancing detection of molecular chirality, is expected to be of large importance for, e.g., discrimination of enantiomers in biology or medicine [9,10].

A question of essential importance is how to control the optical activity of a single building block, i.e., have independent control over the magnetic response, electric response and magnetoelectric cross coupling or ''bi-anisotropy'' whereby incident electric (magnetic) fields cause a magnetic (electric) polarization in a single building block [11]. For instance, in attempts to reach negative indices, researchers soon found that the archetypical split ring resonator (SRR) has a magnetoelectric response that is undesirable, yet difficult to remove without also losing the magnetic response [12]. Completely opposite to the desire to remove this bi-anisotropy, it has also been realized that all applications exploiting optical activity benefit from strong magnetoelectric coupling. Currently it is unclear if there exists any universal bound to which optical activity can be benchmarked, or conversely, if it is at all possible to avoid bi-anisotropy without also losing the magnetic response [13]. In this Letter, we discuss precisely such a universal bound for magnetoelectric coupling for single scatterers, disentangled from any lattice properties. We claim that Onsager's relations constrain optical activity to always be at this maximum bound for any dipole scatterer based on planar circuit designs, independent of geometrical chirality. Our claim is supported by measurements of the strength of pseudochirality in achiral SRRs at telecom wavelengths, and rigorous full-wave calculations [14] to retrieve cross sections and polarizabilities for various metamaterial scatterers [see Figs. 1(a) and 1(b)].

The central quantity in this Letter is the polarizability tensor $\boldsymbol{\alpha}$ that quantifies the magnetic response α_H, electric response α_E and magnetoelectric cross coupling (bi-anisotropy) α_C to the electric $\boldsymbol{E}$ or magnetic $\boldsymbol{H}$ component of the incident light, intrinsic to a single metamaterial building block according to [11,13]:

$$\begin{pmatrix} \mathbf{p} \\ \mathbf{m} \end{pmatrix} = \begin{pmatrix} \boldsymbol{\alpha}_E & i\boldsymbol{\alpha}_C \\ -i\boldsymbol{\alpha}_C^T & \boldsymbol{\alpha}_H \end{pmatrix} \begin{pmatrix} \mathbf{E} \\ \mathbf{H} \end{pmatrix}. \tag{1}$$

For molecules, optical activity occurs in this polarizability tensor as very weak cross coupling, i.e., a perturbative $\alpha_C H \approx 10^{-3}\alpha_E E$, while $\alpha_H \approx 0$ [4]. In contrast, the paradigm of metamaterials is that a single scatterer acquires a magnetic dipole moment $\mathbf{m}$ at least comparable to the electric moment $\mathbf{p}$, with α_E, α_H, and possibly α_C of the same order, which all derive from a single resonance [15]. In order to quantify the polarizability for the canonical SRR, we performed transmission measurements as well as full-wave calculations. For the experiments we fabricated Au SRRs arranged in square arrays on glass substrates by

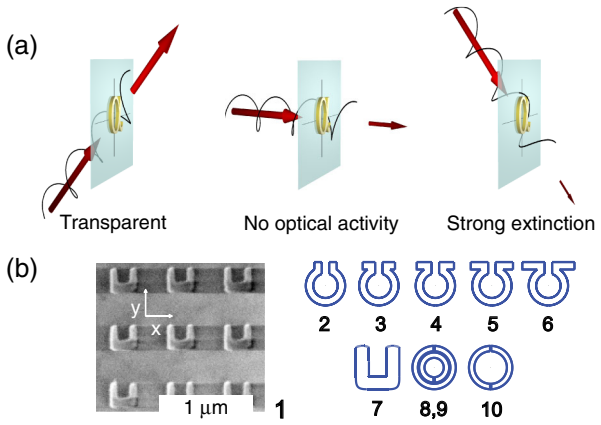

FIG. 1 (color online). (a) Any scatterer α with nonzero electric and magnetic polarizability shows oblique incidence optical activity, with transparency for one handedness of incident light at off-angles, and maximum extinction when the incident beam is rotated by 90°. At normal incidence, the scatterer shows no optical activity. (b) Common planar scatterers for which we verify optical activity: (1) scanning electron micrograph of $230 \times 230 \times 30$ nm Au SRRs. Structures (2)–(6): Ω particles of varying arm length. Structure (7) model for SRR in (1). Structure (8,9,10): double SSR and double-gap SSR [14].

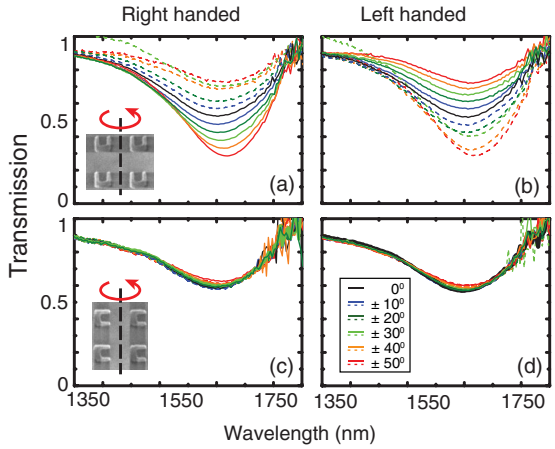

FIG. 2 (color online). Transmission spectra from a periodic square array of 230×230 nm SRRs with $d = 530$ nm. The spectra were taken as a function of angle of incidence, where dashed curves denote negative angles, and solid curves positive angles with respect to the sample normal. (a),(c) and (b),(d) are transmission spectra shown for right- and left-handed circularly polarized illumination. Insets in (a),(c) show the axis over which we rotated the sample for (a),(b), respectively, (c),(d), taking the fixed incident k vector as pointing through the page.

electron beam lithography (e-beam), resonant at telecom wavelengths [16,17]. Figure 1(b) shows a scanning electron micrograph of a SRR array with 530 nm lattice spacing, which is so dilute that coupling between SRRs is small [17], yet so dense that no grating diffraction occurs. Each SRR measures $230 \times 230 \times 30$ nm, with a gap between the arms that is 100 nm wide and 145 nm deep. We record transmission by illuminating the sample with a narrow band of frequencies, selected from a supercontinuum laser (Fianium), using an acousto-optical tunable filter (Crystal Technologies) with a bandwidth of 1–2 nm [18]. The beam is chopped for lock-in detection on an InGaAs photodiode. We circularly polarize the incident beam using a broadband quarter-wave plate, and weakly focus onto the sample ($f = 100$ mm). Light is collected with a low NA collection lens ($f = 20$ mm), and passed through a telescope and pinhole to ensure spatial selection from within a 200×200 μm^2 e-beam write field, as monitored by an InGaAs camera. A motorized sample rotation stage allows transmission measurements versus incident angle relative to the sample normal.

Figure 2 shows transmission versus wavelength for left and right-handed circularly polarized incident light, for incidence angles from −50° to +50°. Figure 2(a) shows data when the angle is varied by rotating the SRRs around their mirror axis y. At normal incidence, the magnetic LC resonance is evident around 1600 nm wavelength as a minimum in transmission. As opposed to the deep minima usually reported for linear, x-polarized transmission (E along the gap), the transmission dip is shallow since our lattice is dilute and the LC resonance is associated only with E_x and H_z, and completely transparent for E_y. As the incidence angle is moved away from the normal, the excitation also offers H_z as a driving field, a quarter wave out of phase with E_x. A very clear asymmetry around the normal develops. For right-handed light the transmission minimum becomes continuously shallower towards negative angles, and the sample is nearly transparent for −50°. In contrast, the transmission minimum significantly deepens from 28% to 75% towards large positive angles. The asymmetry with incidence angle is mirrored for opposite handedness [Fig. 2(b)], consistent with oblique incidence optical activity. Linearly polarized transmission is symmetric around normal incidence (not shown).

The fact that optical activity is symmetry allowed even for lattices containing 2D nonchiral objects aligned with the lattice symmetry, was already reported as "extrinsic chirality" by Plum *et al.* [6], and much earlier by Verbiest *et al.* [3] for achiral molecular thin films. For molecular and metamaterial systems alike, symmetry arguments [4] distinguish between allowed and forbidden effects without quantifying the strength of optical activity. It is the express aim in this Letter to understand its huge strength for metamaterials, i.e., what the single element polarizability is that leads to the strong optical activity. We exclude the array structure factor as the cause of handed behavior [19], as the optical activity disappears when we rotate the SRRs by 90° in the sample plane [Figs. 2(c) and 2(d)]. We hence conclude that the single SRR polarizability must contain the strong "pseudochirality" that is expressed as huge circular dichroism contrast in the extinction cross section, despite SRRs being neither 2D nor 3D chiral. Qualitatively, the LC description of a single SRR indeed contains optical activity under oblique incidence. Charge motion is set by

$\dot{q} = (i\omega L + R + 1/i\omega C)^{-1}[i\omega\mu_0 A H_z + E_x t]$, where L is the inductance, C the capacitance, R the Ohmic resistance, t the capacitor plate gap and A the enclosed area. Full transparency despite the presence of suitable driving E_x along the gap and H_z through the split ring occurs when $i\omega\mu_0 A H_z = -E_x t$. Conversely, optimum driving of a SRR benefits from an opposite quarter-wave phase difference between E_x and H_z so that $[i\omega\mu_0 A H_z + E_x t]$ has maximum magnitude. Circular polarization at oblique incidence provides the required quarter-wave phase difference between E_x and H_z. Alternative to explanation via H_z and E_x, one could explain the handed behavior in Figs. 2(a) and 2(b) as a response to $\partial_x E_y$, since sample rotation introduces a phase gradient between the two arms that reverses with handedness, and rotation angle. In Figs. 2(c) and 2(d), no such gradient is induced, so no optical activity is observed. The explanations are equivalent since $H = \nabla \times E$.

We quantify the polarizability tensor from the data by analyzing the effective extinction cross section per SRR defined as $\sigma_{R,L} = (1 - T_{R,L})d^2$, where d is the lattice pitch and $T_{R,L}$ is the minimum in transmission for right and left-handed circularly polarized light [17]. Figure 3 shows that this *effective* extinction cross section varies between 0.07 and 0.16 μm^2 as the angle is swept from $\pm 50°$ to $\mp 50°$ (mirrored dependence for opposite handedness). For a single magnetoelectric dipole scatterer [13] predicts the extinction cross section generally depends on angle θ as

$$\sigma_{R,L}(\theta) = \sigma_- + (\sigma_+ - \sigma_-)[1 + \cos(2(\theta \pm \theta_0))]/2. \quad (2)$$

Measurements on a single object would provide the electrodynamic [20] α_E through the normal incidence extinction $\sigma_{R,L}(0) = 2\pi k \mathrm{Im}\alpha_E$, while the maximum and minimum attained extinction $\sigma_\pm$ encode electrodynamic polarizability eigenvalues via $\sigma_\pm = \pi k \mathrm{Im}(\alpha_E + \alpha_H \pm \sqrt{(\alpha_E - \alpha_H)^2 + 4\alpha_C^2})$. Such a fit of the single object extinction to the measured effective extinction would provide $\alpha_E = 4.1$ V, $\alpha_H = 3.6$ V and $\alpha_C = 1.4$ V expressed in units of the geometrical volume of the SRR ($V = 0.0012$ μm^3). However, in a lattice of SRRs, the response is modified by coherences such that $(\mathbf{p}, \mathbf{m})^T = 1/[\boldsymbol{\alpha}^{-1} - \mathcal{G}](\mathbf{E}, \mathbf{H})^T$, where a lattice sum Green function $\mathcal{G}$ renormalizes the polarizability [21]. We calculate lattice transmission by rigorous electrodynamic lattice sums involving all multiple-scattering interactions between SRRs [21]. Consistent with our data, the calculated transmission shows strong optical activity under oblique incidence. We extract $\alpha_E = 6.4$ V, $\alpha_H = 0.9$ V, $\alpha_C = 2.1$ V at $\lambda = 1600$ nm from a comparison to data, highlighting that the response of SRR arrays is consistent with remarkably strong magnetoelectric cross coupling.

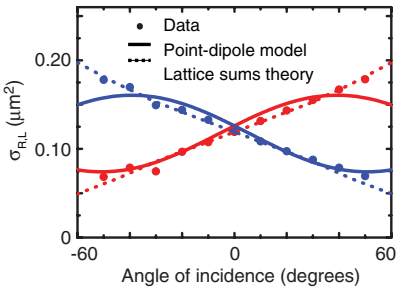

FIG. 3 (color online). Circles: effective extinction per SRR from transmission data. Solid line: single scatterer extinction cross section expected in a dipole model. Dashed line: lattice sum calculation for a square array with pitch $d = 530$ nm.

In Ref. [13] we analyzed how electrodynamic scatterers with arbitrary polarizabilities of the form in Eq. (1) scatter. In that work, we realized that once one applies the optical theorem to a planar scatterer (in-plane $\mathbf{p}$, out-of-plane $\mathbf{m}$), $\bar{\alpha}_C \leq \sqrt{\bar{\alpha}_E \bar{\alpha}_H}$ appears as the maximum value that $\bar{\alpha}_C$—the crosscoupling after taking a common resonant frequency factor out of Eq. (1) [15]—can possibly attain to avoid violation of energy conservation. Here we claim that *any* planar circuit-derived scatterer is necessarily exactly at this upper bound, i.e., at maximum cross coupling. To prove this assertion we analyze a generic model for the polarizability of a planar scatterer under two general assumptions: (1) a linear response and (2) that an electric and magnetic dipole response originate from the *same* equation of motion for charge q moving through the scatterer. Linear response implies $q = C_E(\omega)E + C_H(\omega)H$, where E (H) is in the plane (perpendicular to the plane) of the scatterer. Since $\mathbf{p}$ and $\mathbf{m}$ both derive from the same charge motion, $\mathbf{p} = A_p q$ and $\mathbf{m} = A_m \dot{q} = i\omega A_m(\omega) q$, where A_p and A_m are geometry-dependent constants that were evaluated for some specific circuits in [11]. One now finds the electrostatic circuit polarizability as

$$\boldsymbol{\alpha}_0 = \begin{pmatrix} A_p C_E(\omega) & A_p C_H(\omega) \\ i\omega A_m C_E(\omega) & i\omega A_m C_H(\omega) \end{pmatrix}. \quad (3)$$

For reciprocal materials, Onsager's relations constrain $\boldsymbol{\alpha}_E$ and $\boldsymbol{\alpha}_H$ to be symmetric, as well as requiring $A_p C_H(\omega) = -i\omega A_m C_E(\omega)$. Taking out a common frequency factor $\mathcal{L}(\omega) \propto C_E(\omega)$ that describes the circuit resonance, one finds that α_0 always take the form [15]

$$\boldsymbol{\alpha}_0 = \mathcal{L}(\omega) \begin{pmatrix} \bar{\alpha}_E & i\omega\sqrt{\bar{\alpha}_E \bar{\alpha}_H} \\ -i\omega\sqrt{\bar{\alpha}_E \bar{\alpha}_H} & \omega^2 \bar{\alpha}_H \end{pmatrix}. \quad (4)$$

The surprise is that Onsager constraints *leave no freedom* to choose the off-diagonal coupling $\bar{\alpha}_C$. Any planar circuit element is cross coupled, with cross coupling $\bar{\alpha}_C = \sqrt{\bar{\alpha}_E \bar{\alpha}_H}$. Combining this finding with our result from Ref. [13] we conclude that *any* planar circuit-derived scatterer is not just cross coupled, but that this coupling is at the maximum cross coupling limit. Maximum cross coupling means one vanishing eigenpolarizability $\alpha_- = 0$, hence complete transparency of the scatterer for one handedness under oblique incidence, i.e., huge optical activity.

Based on our experiment, we can now assess whether the strong cross coupling in real scatterers is indeed

close to the predicted maximum. From the polarizability we extracted from the very strong circular polarization contrast in extinction in Fig. 3 we indeed find almost maximum cross coupling, since $\alpha_C \approx 0.88\sqrt{\alpha_E \alpha_H}$. Furthermore, we use full-wave simulations to examine the polarizability, and pseudochirality in extinction of many scatterers. We use 3D Surface Integral Equation (SIE) calculations [14], to obtain full-wave solutions for archetypical metamaterial scatterers including SRRs, Omega particles with straight legs of different length, double SRRs and double-gap rings as shown in Fig. 1(b). We calculate scattering cross sections and polarizability tensors independently from each other. To extract the polarizability, we excite the same scatterer with six linearly independent illumination conditions, obtained as counterpropagating linearly polarized beams set in (out of) phase to yield just electric (magnetic) Cartesian excitation. We project the calculated scattered E-field evaluated on a spherical surface around the scatterer on vector spherical harmonics to retrieve $\mathbf{p}$ and $\mathbf{m}$ [22]. As a consistency check on the polarizability retrieved by matrix inversion we verify the Onsager constraints, which are not *a priori* assumptions in the retrieval. We summarize results for all scatterers in a "master plot" that allows comparison independent of scatterer size. The scatterers are shown in Fig. 1(b). As a first dimensionless variable we use $\xi = (\alpha_E - \alpha_H)/(\alpha_E + \alpha_H)$, which equals ± 1 for purely electric (magnetic) scatterers, and 0 for equal electric and magnetic polarizability. As a dimensionless second variable we take the normalized cross coupling $\eta = \alpha_C/(\alpha_E + \alpha_H)$. The locus of maximum cross coupling is the ellipse $\eta = \sqrt{1 - \xi^2}/2$. Figure 4 shows that most metamaterial scatterers we analyzed have ξ well away from 1, indicating significant magnetic polarizability. Furthermore all particles are essentially on the locus of maximum cross coupling, confirming our claim that bi-anisotropy is ubiquitous.

As third axis for the master plot we use a measure for optical activity in scattering. All scatterers we simulated show an angular dependence of the scattering cross section of the form in Eq. (2). The dimensionless parameter $\Psi = |\sigma_R - \sigma_L|/(\sigma_R + \sigma_L)$ evaluated at 45° incidence angle quantifies the maximum attained difference in extinction $|\sigma_R - \sigma_L|$ (maximal always at 45°) normalized to (twice) the angle-averaged extinction cross section $\sigma_+ + \sigma_-$. Figure 4 shows Ψ versus ξ and η as predicted by point scattering theory. Evidently, optical activity is expected to be absent for zero cross coupling, and to increase monotonically as cross coupling increases. Very strong contrast in extinction per building block is expected along most of the locus of maximum cross coupling, vanishing only for purely electric, and purely magnetic dipole scatterers ($\xi = \pm 1$). The full-wave simulations show that all the commonly used metamaterial scatterers exhibit strong optical activity in surprisingly good agreement with the dipole model given that the circuit approximation, and the

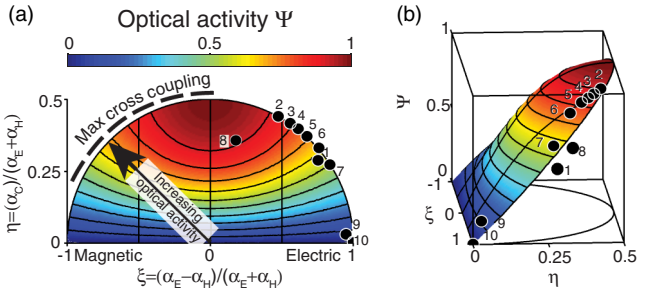

FIG. 4 (color online). Master diagrams summarizing optical activity and bi-anisotropy mapped as a function of $\xi = (\alpha_E - \alpha_H)/((\alpha_E + \alpha_H)$ and $\eta = (\alpha_C)/(\alpha_E + \alpha_H)$. All structures we tested [data points, numbered as in Fig. 1(b)] are close to the locus of maximum cross coupling (ellipse), except (8). The color scale shows optical activity contrast Ψ, in the dipole approximation (color scale) and for tested structures (dots). Panel (b) is a 3D representation of (a).

neglect of multipoles and retardation in Eq. (4) are very coarse assumptions. Freedom to deviate significantly from the dipole model requires multiple overlapping resonances in a single scatterer. Indeed, the most noted deviations occur for the object (8,9) which has two hybridized resonances of separate parts. Earlier findings based on symmetry arguments proposed that extrinsic 3D chirality requires loss [6]. We find that optical activity is in fact ubiquitous, irrespective of absorption. Cancellation of optical activity for zero absorption noted by [6] does not occur in $\boldsymbol{\alpha}$ but occurs in special cases constrained by additional symmetries, such as wave vector conservation in nondiffracting periodic systems.

To conclude, we have shown that planar metamaterial scatterers that rely on a single resonance to generate a simultaneous electric and magnetic response are maximally bi-anisotropic and strongly optically active, whether they exhibit geometrical chirality or not. Optical activity, in achiral structures was already known to be allowed by symmetry [3,6]. Our finding that this effect is inevitably maximally large for metamaterials, rather than being a perturbatively weak cross-polarizability [4] as for molecules, has important implications for controlling bi-anisotropy in metamaterials, since they imply that it is fundamentally impossible to independently control bi-anisotropy for single resonant objects. The only route to avoid bi-anisotropy in lattices of resonators is to use heterogeneous lattices that contain distinct, or multiresonant elements (e.g., double SSRs in Fig. 4) to independently generate ϵ and μ, or to use lattices of effectively larger "supercells" with rotated copies of the same building block to cancel off-diagonal coupling. Our results also hold important promise for enhancing far-field or near-field chirality [9] in scattering applications. Since maximum cross coupling is ubiquitous, optical activity is a very robust phenomenon that is easily extended to, e.g., finite clusters, random assemblies, or multielement antennas. For instance, we predict that chiral variants of the plasmon

Yagi-Uda antenna will generate or selectively enhance circularly polarized single emitters. Enhanced chirality in the near-field will promote discrimination between enantiomers on the single molecule level using the fact that chiral fluorophores have enantioselective absorption cross sections. Also, near-field chirality can result in enantioselective resonance shifts for nonfluorescent species [10,11]. Finally, our work raises the interesting question if and under which conditions the maximally strong coupling of classical magnetoelectric scatterers can be translated to molecular wave functions, to optimize per molecule optical activity.

We thank Huib Bakker and Ad Lagendijk for fruitful discussions. This work is part of the research program of the ''Stichting voor Fundamenteel Onderzoek der Materie (FOM),'' which is financially supported by the ''Nederlandse Organisatie voor Wetenschappelijk Onderzoek (NWO).''

*i.sersic@amolf.nl
URL: http://www.amolf.nl/research/resonant-nanophotonics/

[1] V. G. Veselago, Sov. Phys. Usp. **10**, 509 (1968); J. B. Pendry, Phys. Rev. Lett. **85**, 3966 (2000); J. B. Pendry, Phys. World **14**, 47 (2001); C. M. Soukoulis, S. Linden, and M. Wegener, Science **315**, 47 (2007); V. M. Shalaev, Nature Photon. **1**, 41 (2007).

[2] J. B. Pendry, D. Schurig, and D. R. Smith, Science **312**, 1780 (2006); U. Leonhardt, *ibid.* **312**, 1777 (2006); D. Schurig, J. J. Mock, B. J. Justice, S. A. Cummer, J. B. Pendry, A. F. Starr, and D. R. Smith, *ibid.* **314**, 977 (2006).

[3] T. Verbiest, M. Kauranen, Y. Van Rompaey, and A. Persoons, Phys. Rev. Lett. **77**, 1456 (1996); T. Verbiest, M. Kauranen, and A. Persoons, *ibid.* **82**, 3601 (1999).

[4] L. D. Barron, *Molecular Light Scattering and Optical Activity* (Cambridge University Press, Cambridge, England, 2004), 2nd ed.

[5] A. Drezet, C. Genet, J.-Y. Laluet, and T. W. Ebbesen, Opt. Express **16**, 12 559 (2008); V. K. Valev, N. Smisdom, A. V. Silhanek, B. De Clercq, W. Gillijns, M. Ameloot, V. V. Moshchalkov, and T. Verbiest, Nano Lett. **9**, 3945 (2009); Y. Gorodetsky, N. Shitrit, I. Bretner, V. Kleiner, and E. Hasman, *ibid.* **9**, 3016 (2009); S. Zhang, Y.-S. Park, J. Li, X. Lu, W. Zhang, and X. Zhang, Phys. Rev. Lett. **102**, 023901 (2009); E. Plum, J. Zhou, J. Dong, V. A. Fedotov, T. Koschny, C. M. Soukoulis, and N. I. Zheludev, Phys. Rev. B **79**, 035407 (2009); J. Zhou, J. Dong, B. Wang, T. Koschny, M. Kafesaki, and C. M. Soukoulis, *ibid.* **79**, 121104 (2009); J. K. Gansel, M. Thiel, M. S. Rill, M. Decker, K. Bade, V. Saile, G. von Freymann, S. Linden, and M. Wegener, Science **325**, 1513 (2009); M. Decker, R. Zhao, C. M. Soukoulis, S. Linden, and M. Wegener, Opt. Lett. **35**, 1593 (2010); Z. Li, R. Zhao, T. Koschny, M. Kafesaki, K. B. Alici, E. Colak, H. Caglayan, E. Ozbay, and C. M. Soukoulis, Appl. Phys. Lett. **97**, 081901 (2010).

[6] E. Plum, X.-X. Liu, V. A. Fedotov, Y. Chen, D. P. Tsai, and N. I. Zheludev, Phys. Rev. Lett. **102**, 113902 (2009); E. Plum, V. A. Fedotov, and N. I. Zheludev, J. Opt. **13**, 024006 (2011).

[7] J. B. Pendry, Science **306**, 1353 (2004).

[8] R. Zhao, J. Zhou, Th. Koschny, E. N. Economou, and C. M. Soukoulis, Phys. Rev. Lett. **103**, 103602 (2009).

[9] Y. Tang and A. E. Cohen, Phys. Rev. Lett. **104**, 163901 (2010).

[10] Z. Fan and A. O. Govorov, Nano Lett. **10**, 2580 (2010); E. Hendry, T. Carpy, J. Johnston, M. Popland, R. V. Mikhaylovskiy, A. J. Lapthorn, S. M. Kelly, L. D. Barron, N. Gadegaard, and M. Kadodwala, Nature Nanotech. **5**, 783 (2010); Y. Tang and A. E. Cohen, Science **332**, 333 (2011).

[11] I. V. Lindell, A. H. Sihvola, S. A. Tretyakov, and A. J. Viitanen, *Electromagnetic Waves in Chiral and Bi-Isotropic Media* (Artech House, Norwood, MA, 1994); S. A. Tretyakov, C. R. Simovski, and A. A. Sochava, in *Advances in Complex Electromagnetic Materials*, edited by A. Priou, A. Sihvola, S. Tretyakov, and A. Vinogradov, NATO ASI Series High Technology, Vol. 28 (Kluwer Academic Publishers, Dordrecht, 1997).

[12] N. Katsarakis, T. Koschny, M. Kafesaki, E. N. Economou, and C. M. Soukoulis, Appl. Phys. Lett. **84**, 2943 (2004).

[13] I. Sersic, C. Tuambilangana, T. Kampfrath, and A. F. Koenderink, Phys. Rev. B **83**, 245102 (2011). The appendix specifies the units also used in this Letter.

[14] A. M. Kern and O. J. F. Martin, J. Opt. Soc. Am. A **26**, 732 (2009). We use tabulated optical constants for gold [20], and the following dimensions: inner/outer radii in μm 0.74/1.19 (2–6), 1.6/2.5 and 2.7/3.6 (8), 2.7/3.6 (10), with a gap of 450 nm, respectively, 200 nm for structures (2–6) respectively, (10). For scatterers (2–6) we increased the outer arm length from 0 to 900 nm. Scatterer thickness is 30 nm throughout. The resonance wavelengths of the scatterers in μm are 1.600, 15.40, 16.06, 16.41, 16.80, 17.58, 1.544, 62.50, 23.25, and 16.50 for structures (1–10). Resonances (8,9) are two resonances in one structure.

[15] In the static limit α_E, α_H and α_C are real and Ohmic loss appears in $\mathcal{L}$ in Eq. (4). The addition of radiation damping sets α_E, α_H and α_C to be complex quantities even in absence of Ohmic damping [13].

[16] C. Enkrich, M. Wegener, S. Linden, S. Burger, L. Zschiedrich, F. Schmidt, J. F. Zhou, Th. Koschny, and C. M. Soukoulis, Phys. Rev. Lett. **95**, 203901 (2005).

[17] I. Sersic, M. Frimmer, E. Verhagen, and A. F. Koenderink, Phys. Rev. Lett. **103**, 213902 (2009).

[18] I. Sersic, C. Tuambilangana, and A. F. Koenderink, New J. Phys. **13**, 083019 (2011).

[19] B. Gompf, J. Braun, T. Weiss, H. Giessen, M. Dressel, and U. Hübner, Phys. Rev. Lett. **106**, 185501 (2011).

[20] We define a dynamic α by adding radiation damping $\mathrm{inv}(\alpha) = \mathrm{inv}(\alpha_0) - i(2/3)k^3\mathbb{I}$ to a static α_0 [13] with Lorentzian resonance $\mathcal{L}(\omega)$ centered at 1600 nm, and with damping rate of gold $\gamma = 1.25 \times 10^{14}\ \mathrm{s}^{-1}$ from *Handbook of Optical Constants of Solids*, edited by E. D. Palik (Academic, Orlando, FL, 1985).

[21] F. J. García de Abajo, Rev. Mod. Phys. **79**, 1267 (2007).

[22] S. Mühlig, C. Menzel, C. Rockstuhl, and F. Lederer, Metamaterials **5**, 64 (2011).